Digest Journal of Nanomaterials and Biostructures Vol. 7, No. 1, January - March 2012, p. 23 - 32

MAIN REFRACTIVE INDICES OF NEMATIC LIQUID CRYSTALS DETERMINED BY INTERFEROMETRIC METHOD IN CONOSCOPIC ILLUMINATION

I. DUMITRASCU*, LEONAS DUMITRASCU[a], D. – O. DOROHOI[b]
"Al. I. Cuza" University, Faculty of Physics, 11 Carol I Blv. RO-700506, Iasi, Romania
[a]*Instituto Superior Tecnico, Av. Rovisco Pais, 1, 1049-001 Lisabona, Portugalia*
[b]*"Petru Poni" Institute of Macromolecular Chemistry, 41A Grigore Ghica Voda Alley,Iasi-700487, Romania*

A conoscopic method to determine the main refractive indices of a uniaxial anisotropic substance (anisotropic plate or liquid crystalline layer) with its optical axis parallel to the cutting surface is developed in this paper. The values of the birefringence for blue radiation emitted by a Hg light source are determined here for a lyotropic liquid crystal layer in planar orientation. To check the validity of the proposed method, the results obtained are compared with those obtained by supplementary measurements at a Rayleigh interferometer and from the channeled spectra.

(Received October 31, 2011; Accepted January 10, 2012)

Keywords: Polarizing Microscope, Poly-phenyl methacrylic ester of cetyloxybenzoic acid in Tetrachloromethane, Main Refractive Indices, Birefringence

1. Introduction

Conoscopic interference is a commonly used optical technique in polarizing microscopy with applications in areas such as: material science, mineralogy and biological studies [1]. It permits to characterise a sample from the point of view of its anisotropy.

The principle is based on the optical birefringence exhibited by various anisotropic crystals (or other anisotropic layers such as the liquid crystalline one). When linearly polarized light is incident on an anisotropic layer at an arbitrary angle, it decomposes into two mutually orthogonal components which travel through the anisotropic layer at different phase velocities. After the recombination of the two components, at the exit from the layer, the transmitted light is usually elliptically polarized due to the cumulated phase retardation difference. The elliptical polarization can be analyzed by a polarizer. For cones of incident light, the resulting families of interference fringes are characteristic of the layer type; they depend on the thickness and on the birefringence of the anisotropic sample [1,2].

For quantitative studies of the interference figures obtained with the polarizing microscope under conoscopic illumination, the angles between the directions corresponding to the maxima (or minima) of interference need to be determined. In the classical techniques, the angles are measured with a goniometric system by rotating (in the spindle stage techniques [3,4]) or by tilting (in the tilting stage techniques [5]) the normal direction on the surface sample so that the direction of the interference maxima (or minima) becomes parallel to the microscope tube axis. Both techniques require the use of some additional components that increase the complexity of the experimental installation and errors can appear for each studied direction both in reading the goniometric scale and in appreciating the good alignment between the examined direction and the microscope tube

* Corresponding author: ddorohoi@uaic.ro

axis [5-7].

The technique presented in this paper is based on the computational processing of the conoscopic interference figures captured with a digital camera so it does not require reading a goniometric scale to determine the direction for each interference maxima (or minima).

The equations used to express the interference maxima or minima positions are based on the information related to the light propagation in two particular planes: the plane that contains the optical axis and the plane perpendicular to it. If the camera used has a good optical zoom (15X or 20X) and its sensor is one with a high resolution (~4000×3000 pixels or greater), the precision of the method can be considerably increased.

In order to obtain the conoscopic interference figures, samples with high anisotropy are necessary. The samples must be cut in the correct orientation (or with optical axis parallel or perpendicular to the glass walls of the cell in which liquid crystal is kept) and with the thickness greater than a minimum value.

To illustrate the proposed technique we intend to determine the main refractive indices and the birefringence for a mixture of poly-(phenyl-methacrylic) ester of cetyloxybenzoic acid (PPMAECOBA) $10^{-2}\ \mathrm{g/cm^3}$ in tetra chloromethane (TCM). The formula of the polymer is given in Fig.1a. The mixture PPMAECOBA with TCM possesses properties corresponding to a lyotropic nematic liquid crystal (NLC). The NLC was kept into a special cell shown in Fig. 1 (b) [8,9]. This cell consists of two glass plates separated by four spacers with a calibrated height $h = 14 \times 10^{-6} m$ (determining the thickness of the NLC anisotropic layer).

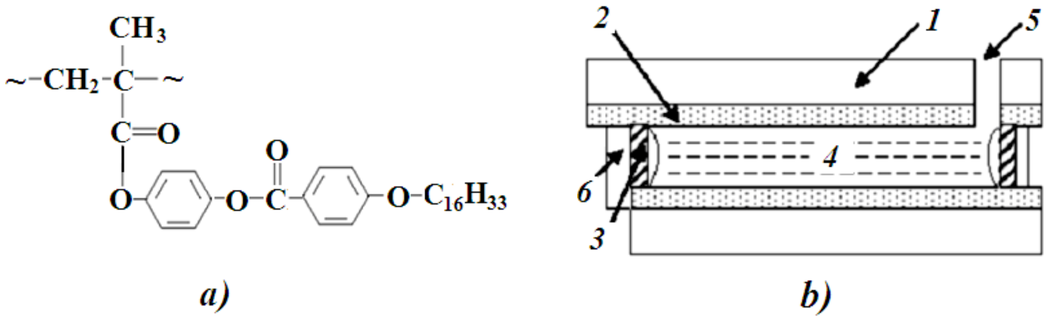

Fig. 1. (a) PPMAECOBA structural formula; (b) The cell containing the lyotropic NLC: 1 - glass plate; 2 – molecular orientation layer (solution of 5% lecithin in water); 3– spacers; 4 – NLC; 5 – filling aperture; 6 – epoxy resin.

To obtain a NLC layer in uniform planar orientation (with director parallel to the cell walls), the dominant orientation of the long molecular axes was mechanically ensured. Additionally, the interior walls of the cell were covered with an orientation layer of lecithin. The orientation of the side chains of the polymer was marked in order to show the orientation of the optical axis (Oc - Figs. 2 (a) and (b)). After filling, the exterior margins of the cell containing liquid crystal were sealed with epoxy resin.

2. Theoretical background

Let us consider a cell of a thickness h filled with a nematic liquid crystal having the director **n** parallel to Oc axis (optical axis) and illuminated by a divergent beam of monochromatic radiation (Fig. 2 (a)). Let also suppose that the cell is placed between two crossed polarizers (the polarizer P and the analyzer A) with their transmission directions at $\varphi = 45^{o}$ to the optical axis (Oc) of the anisotropic layer (Fig. 2 (b)).

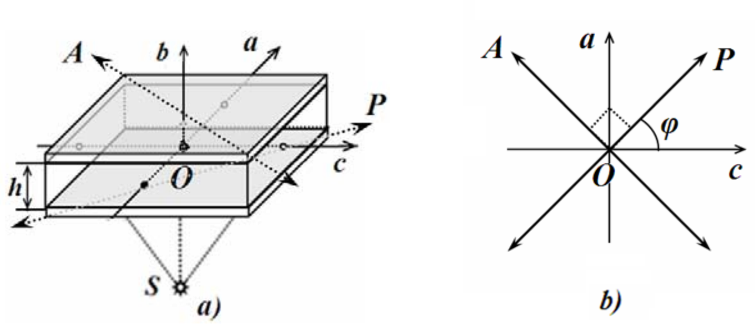

Fig. 2. (a) Liquid crystal cell placed between two crossed polarizers; (b) Relative orientation of the basic directions of anisotropic layer and of the polarizers'transmission directions.

The intensity of the transmitted beam at the exit from the device can be expressed by the following equation [5]:

$$I_A = \frac{1}{2} I_o \sin^2\left(\frac{\pi \cdot (\Delta)}{\lambda_o}\right) \tag{1}$$

In equation (1), λ_o is the wavelength of the monochromatic radiation and (Δ) represents the pathway difference between the ordinary and extraordinary rays corresponding to each incidence considered (Fig. 3 (a)).

From equation (1), it results that the pathway difference (Δ) corresponding to the passage from a maxim to a neighbouring minim is $\lambda_{\mathbf{o}}/2$.

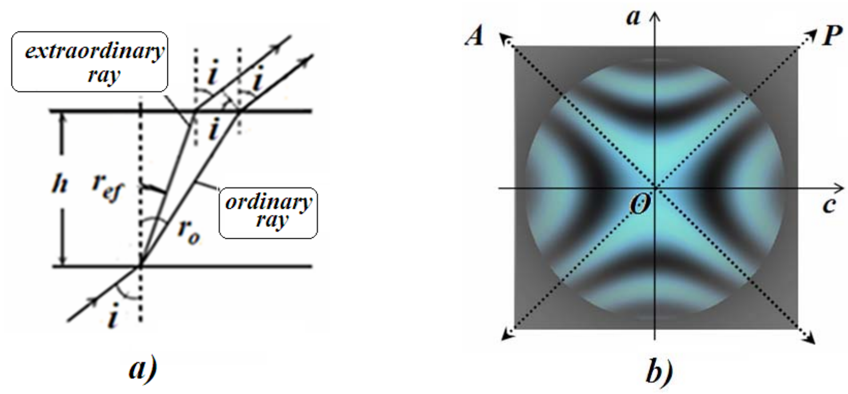

Fig. 3. (a) Ordinary and extraordinary rays in the NLC layer; (b) Image of the interference figure obtained with a polarizing microscope.

When the optical axis of the NLC layer is contained in the cell walls, the radiant energy distribution in the image obtained with the polarizing microscope has the aspect from Fig. 3 b.

The pathway differences $(\Delta)_{||}$ and $(\Delta)_{\perp}$ between the rays propagating in a plane parallel to optical axis (Obc) and, respectively, in the plane perpendicular to the optical axis (Oab) can be expressed by the equations ([10,11]:

$$\begin{cases} (\Delta)_{||} = h(n_e - n_o)\sqrt{1 - \dfrac{\sin^2 i_{m_{||}}}{n_o^2}} \\ (\Delta)_{\perp} = h\left(\sqrt{n_e^2 - \sin^2 i_{m_\perp}} - \sqrt{n_o^2 - \sin^2 i_{m_\perp}}\right) \end{cases} \tag{2}$$

Analyzing equations (2) it results the following properties for the absolute values of the pathway differences $\left|(\Delta)_{\|}\right|$ and $\left|(\Delta)_{\perp}\right|$:

1. At normal incidence (Fig. 4 (a) and (b)):

$$\left|(\Delta)_{\perp}\right|_{(i_{m_\perp}=0)} = \left|(\Delta)_{\|}\right|_{(i_{m_\|}=0)} \tag{3}$$

2. At oblique incidence (Figs. 4 (a) and (b)):

$$\left|(\Delta)_{\perp}\right| > \left|(\Delta)_{\|}\right| \tag{4}$$

3. The absolute value of the pathway difference $\left|(\Delta)_{\perp}\right|$ increases with the increase in the incidence angle $i_{m_\perp}$ (Fig. 4 (a));

4. The absolute value of the pathway difference $\left|(\Delta)_{\|}\right|$ decreases with the increase in the incidence angle $i_{m_\|}$ (Fig. 4 (b));

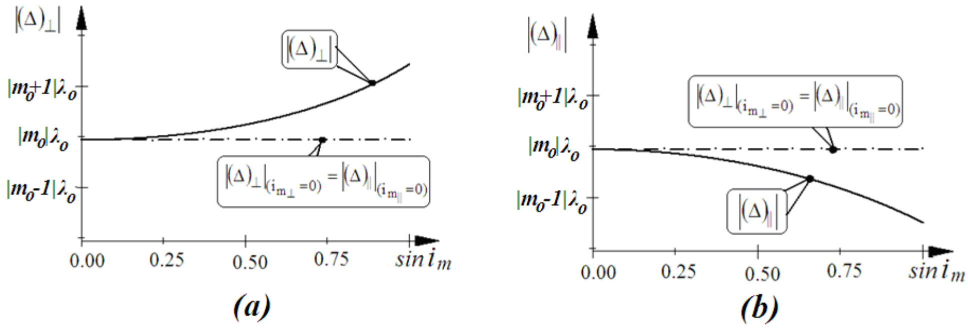

Fig. 4. (a) Plot of the pathway difference $\left|(\Delta)_{\perp}\right|$; (b) Plot of the pathway difference $\left|(\Delta)_{\|}\right|$ (m_o - interference order corresponding to the central part of the interference figure).

2.1 Ordinary refractive index determination

Let be two interference minima situated along the Oc-axis, with consecutive interference orders ($m_\|$) and ($m_\| - 1$) and the maximum between them. Noting by $i_{m_\|}$ and $i_{m_\|-1}$ the incidence angles corresponding to the minima and by $i_{M_\|}$ the incidence angle corresponding to the maximum ($i_{m_\|-1} > i_{M_\|} > i_{m_\|}$), system (6) can be obtained from the first equation (2).

$$\begin{cases} h(n_e - n_o)\left(\sqrt{1-\dfrac{\sin^2 i_{m_\|}}{n_o^2}} - \sqrt{1-\dfrac{\sin^2 i_{M_\|}}{n_o^2}}\right) = \dfrac{\lambda_o}{2} \\ h(n_e - n_o)\left(\sqrt{1-\dfrac{\sin^2 i_{M_\|}}{n_o^2}} - \sqrt{1-\dfrac{\sin^2 i_{m_\|-1}}{n_o^2}}\right) = \dfrac{\lambda_o}{2} \end{cases} \tag{6}$$

Dividing the two equations from (6), one obtains the equation:

$$\sqrt{n_o^2 - \sin^2 i_{m_\|}} + \sqrt{n_o^2 - \sin^2 i_{m_\|-1}} = 2\sqrt{n_o^2 - \sin^2 i_{M_\|}} \tag{7}$$

Equation (7) permits to determine the ordinary refractive index of the studied liquid crystal when the thickness of the layer is unknown.

2.2 Extraordinary refractive index determination

Let us consider the two consecutive maxima of interference ($M_\perp$) and ($M_\perp + 1$) situated along the Oa-axis and the minimum between them (Fig. 3 (b)). By noting with $i_{M_\perp}$ and $i_{M_\perp+1}$ the incidence angles corresponding to the two maxima and with $i_{m_\perp}$ the incidence angle corresponding to the minimum between them $(i_{M_\perp} < i_{m_\perp} < i_{M_\perp+1})$, from the second equation (2), one can obtained the following equation system:

$$\begin{cases} h\left(\left(\sqrt{n_e^2-\sin^2 i_{m_\perp}}-\sqrt{n_o^2-\sin^2 i_{m_\perp}}\right)-\left(\sqrt{n_e^2-\sin^2 i_{M_\perp}}-\sqrt{n_o^2-\sin^2 i_{M_\perp}}\right)\right)=\dfrac{\lambda_o}{2} \\ h\left(\left(\sqrt{n_e^2-\sin^2 i_{M_\perp+1}}-\sqrt{n_o^2-\sin^2 i_{M_\perp+1}}\right)-\left(\sqrt{n_e^2-\sin^2 i_{m_\perp}}-\sqrt{n_o^2-\sin^2 i_{m_\perp}}\right)\right)=\dfrac{\lambda_o}{2} \end{cases} \tag{8}$$

By dividing the equations (6) member to member, equation (9) can be obtained:

$$\begin{aligned} &\left(\sqrt{n_e^2-\sin^2 i_{M_\perp}}-\sqrt{n_o^2-\sin^2 i_{M_\perp}}\right)+\left(\sqrt{n_e^2-\sin^2 i_{M_\perp+1}}-\sqrt{n_o^2-\sin^2 i_{M_\perp+1}}\right)= \\ &2\left(\sqrt{n_e^2-\sin^2 i_{m_\perp}}-\sqrt{n_o^2-\sin^2 i_{m_\perp}}\right) \end{aligned} \tag{9}$$

The main refractive indices of the liquid crystal layer can be determined by using equations (7) and (9).

2.3 Determination of the layer thickness

Let us return to system of equations (8). To determine the thickness of the anisotropic layer one can use the following equations:

$$\begin{aligned} h &= \frac{\lambda_o}{2\left(\left(\sqrt{n_e^2-\sin^2 i_{m_\perp}}-\sqrt{n_o^2-\sin^2 i_{m_\perp}}\right)-\left(\sqrt{n_e^2-\sin^2 i_{M_\perp}}-\sqrt{n_o^2-\sin^2 i_{M_\perp}}\right)\right)} \\ h &= \frac{\lambda_o}{2\left(\left(\sqrt{n_e^2-\sin^2 i_{M_\perp+1}}-\sqrt{n_o^2-\sin^2 i_{M_\perp+1}}\right)-\left(\sqrt{n_e^2-\sin^2 i_{m_\perp}}-\sqrt{n_o^2-\sin^2 i_{m_\perp}}\right)\right)} \end{aligned} \tag{10}$$

The first equation from the system of equations (2) and the thickness h determined with equations (10) allow us to re-compute the values of the birefringence and to verify thus the consistence of the experimental data obtained.

The equations allowing re-evaluating the birefringence values are:

$$\begin{aligned} (n_e-n_o) &= \frac{\lambda_o}{2h\left(\sqrt{1-\dfrac{\sin^2 i_{m_\parallel}}{n_o^2}}-\sqrt{1-\dfrac{\sin^2 i_{M_\parallel}}{n_o^2}}\right)} \\ (n_e-n_o) &= \frac{\lambda_o}{2h\left(\sqrt{1-\dfrac{\sin^2 i_{M_\parallel}}{n_o^2}}-\sqrt{1-\dfrac{\sin^2 i_{m_\parallel-1}}{n_o^2}}\right)} \end{aligned} \tag{11}$$

3. Experimental set-up

The conoscopic interference figures studied in this paper were obtained with a polarizing microscope (Fig. 5 (a)) by applying the common technique described in [3,4, 12].

The captured images were made in the blue radiation ($\lambda_o = 4358.3 \times 10^{-10}$ m) emitted by a Hg discharge lamp.

The condenser aperture diaphragm was fitted to correspond to the numerical aperture of the microscope objective used (in our case an objective with M=40X and $NA_{obj.}$ = 0.95). This choice ensures the maximum resolution for the captured images and permits the use of the equations presented above to make the measurements on the interference figures.

To capture the images of the interference figures the camera objective was fixed coaxially with the microscope ocular. The digital camera used was a Sony Cybershot DSC-H7 with 8.1MP (3264 x 2448 pixels) maxim resolution and 15X optical zoom.

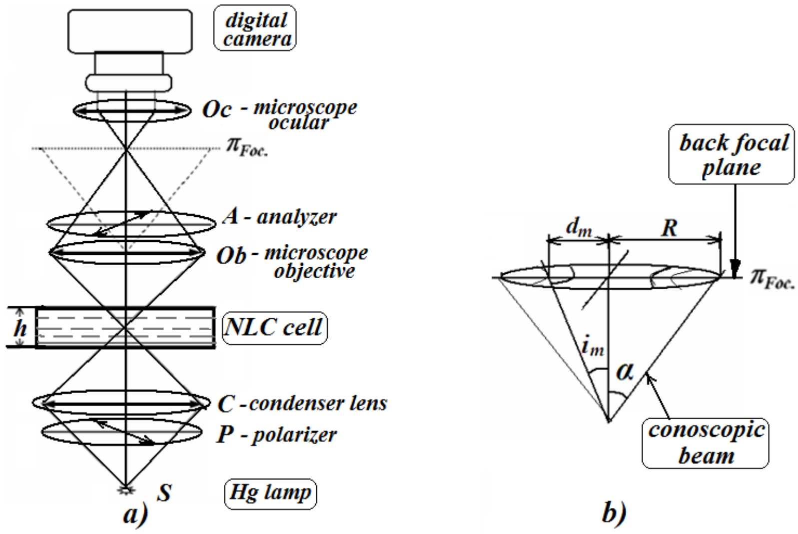

Fig. 5. (a) Simplified optical schema of the polarizing microscope with a digital camera attached. (b) Symbols used in equation (12) for $\sin i_m$ determination.

4. Image processing

For the interference figures obtained with a high-power microscope objective, and enlarged by means of an auxiliary lens [11], the incidence angles i_m should satisfy the following equation (Fig. 5. (b))

$$\sin i_m = \rho_m \sin\alpha; \left(\rho_m = \frac{d_m}{R}\right) \tag{12}$$

In particular, if the angular aperture α corresponds to the numerical aperture of the microscope objective (NA_{obj}), then in equation (12) one can use the definition [12]:

$$\sin\alpha = NA_{obj} \tag{13}$$

The measurements of d_m and R from equation (12) were realized in three steps:

1. The captured images were digitally processed by using the application 3DFieldPro (http://field.hypermart.net/download.htm) as is shown in Figs. 6 (a) and (b). This application permits to draw the light intensity graphics as function of pixels positions and to determine the position corresponding to the interference minima and maxima.
2. The values of $2d_m$ and 2R from the graphics shown in Fig. 6 (b) were measured (in pixels) using the application Get Data Graph Digitizer v. 2.24 (http://getdata-graph-digitizer.com).

According to the ROMM/RIMM RGB colour encoding specifications [13], the maxim numbers of quantization steps for the intensity values are set to: 255, 4095 or 65535 (for 8-, 12-, and 16-bit versions of ROMM/RIMM RGB specification). Because the application 3DFieldPro is compatible with the 16-bit of ROMM/RIMM RGB specification, the width of the interference minima (and maxima) processed with this application can be reduced to a single pixel.

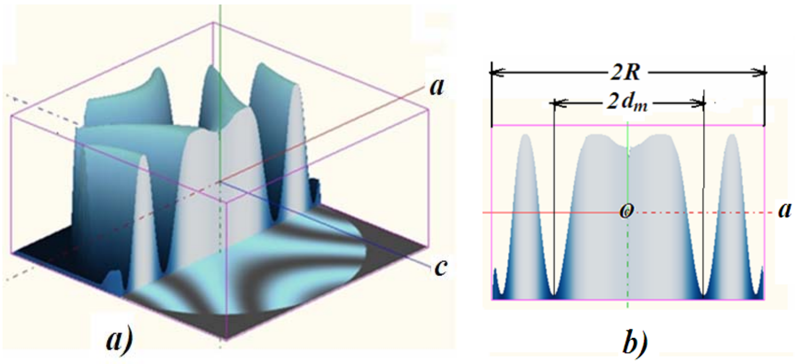

Fig. 6. (a) Section along Oa axis obtained with 3DFielPro application; (b) Determination of the values of $2d_m$ *and* $2R$.

3. In order to increase the precision and the resolution at sub-pixel level, the values of d_m should be statistically estimated for each interference minima and maxima. In the hypothesis that the interference fringes are equilateral hyperbolas [2], the coordinates of the points M_q and M'_q (Fig. 7 (b)) should satisfy the following equation:

$$\frac{x_q^2}{a^2} - \frac{y_q^2}{b^2} = 1 \tag{14}$$

For the crossed polarizers having their transmission directions oriented at $\varphi = 45^{\circ}$ to the optical axis (Oc) of the anisotropic layer (Figs. 2 (b) and 7(b)) it results:

$$a = b = d_m \tag{15}$$

By combining equations (14) and (15) one obtains:

$$d_m = \sqrt{x_q^2 - y_q^2} \tag{16}$$

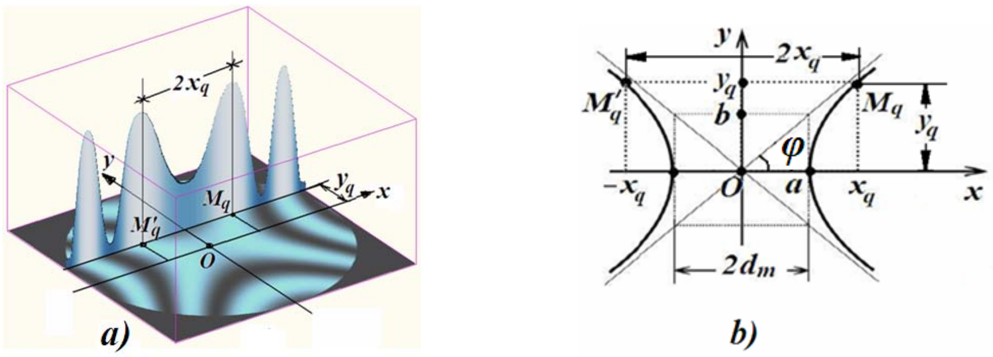

Fig. 7. (a) Section parallel to Ox direction obtained with the application 3DFieldPro for $y_q \neq 0$*; (b) Hyperbola described by equation (14) used for the statistical estimation of* d_m.

5. Results and discussion

The results obtained by applying equation (16) for 15 positions on the hyperbola corresponding to the first interference maxima along the Oa axis are shown in Fig. 8.

The mean value calculated for d_m was in this case $< d_m >= 680.20 \pm 0.05$ pixels .

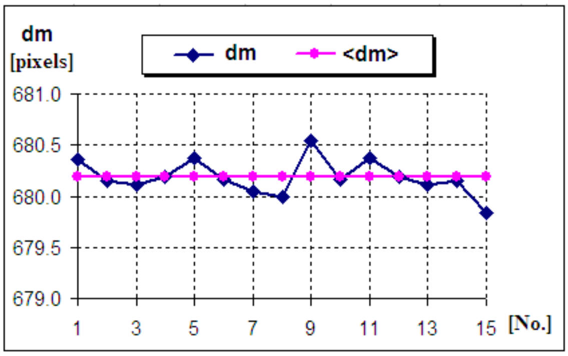

Fig. 8. Example of distribution values of d_m *for the first maxima obtained along the Oa axis.*

The values obtained for $< d_m >$, ρ_m and $\sin i_m$ after the image processing, by using the equation (12) and the values $NA_{obj} = 0.95$ and $R = 1214 \pm 0.1$ pixels, are listed in Table 1.

Table 1. Value of $< d_m >$, ρ_m *and* $\sin i_m$ *obtained for PPMAECOBA in TCM.*

incidence angle	$< d_m >$ [pixels]	ρ_m	$\sin i_m$
$i_{m_{\parallel}-1}$	1042.25	0.85853	0.81560
$i_{M_{\parallel}}$	780.88	0.64323	0.61107
$i_{m_{\parallel}}$	316.84	0.26099	0.24794
$i_{M_{\perp}}$	680.20	0.56029	0.53228
$i_{m_{\perp}}$	974.25	0.80252	0.76239
$i_{M_{\perp}+1}$	1166.27	0.96068	0.91265

The value of the ordinary and extraordinary refractive indices estimated by using the equation (7) and (9) and the data from Table 1 are those listed in Table 2.

Table 2. Value of n_o, n_e, $\Delta n = n_e - n_o$ *obtained for PPMAECOBA in TCM on the basis of equations (7) and (9).*

n_o (Eq. (7))	n_e (Eq. (9))	$\Delta n = n_e - n_o$
1. 6236 ±0.0007	1. 8757±0.0007	0.2521±0.0015

The value of the birefringence and the thicknesses obtained by using the data from Table 1 and the equations (8), (9) and (11) are shown in Table 3.

Table 3. Value of $\Delta n = n_e - n_o$ *estimated by using Eqns. (8) and (9) and (11), respectively, and thickness estimated by Eqn.(10), for PPMAECOBA in TCM.*

No.	$\Delta n = n_e - n_o$ (Eqns. (8) and (9))	h [m] (Eq. (10))	$\Delta n = n_e - n_o$ (Eq. (11))
1.	0.2520±0.0015	$(13.99\pm0.02)\times10^{-6}$	0.2518±0.0015
2.	0.2519±0.0015	$(13.98\pm0.02)\times10^{-6}$	0.2518±0.0015

The estimation of the thickness of the NLC layer is made on the basis of equation (10) and by using the data obtained for the direction of Oa -axis, oriented perpendicular to the optical axis; the results obtained are listed in Table 3. These values are concordant with the calibrated thickness of the cell spacers ($h = (14.00 \pm 0.05)\times 10^{-6}\,\mathrm{m}$).

From Tables 1 and 3 one can see that the birefringence values re-evaluated by applying the equations (11) are in a good accordance with those obtained by applying the equations (8) and (9), and with those obtained by applying other techniques (Rayleigh interferometric technique and channelled spectra technique [8, 9] .

The technique described can be applied only if the thickness of the anisotropic layers is sufficiently high. In order to determine the minimum layer (sample) thickness value, let us analyze the situation in which the registration of two consecutive minima and the maximum between them is made on the direction Oc (optical axis).

The modulus of the pathway difference $\left|(\Delta)_{\|}\right|$ must have a maximum value for the central zone of the interference field, and a minimum value at the periphery. From the equation (1) and the first equation (2) one obtains (17) for two consecutive minima.

$$\begin{aligned}(\Delta)_{\|\max} &= h(n_e - n_o)\sqrt{1-\frac{\sin^2 i_{min}}{n_o^2}} = m_{\|}\lambda_o \\ (\Delta)_{\|\min} &= h(n_e - n_o)\sqrt{1-\frac{\sin^2 i_{max}}{n_o^2}} = (m_{\|}-1)\lambda_o\end{aligned} \tag{17}$$

To obtain at least two interference minima and the maximum between them, the difference $(\Delta)_{\|\max} - (\Delta)_{\|\min}$ must be higher than two semi wave length:

$$(\Delta)_{\|\max} - (\Delta)_{\|\min} \geq m_{\|}\lambda_o - (m_{\|}-1)\lambda_o \geq 2\frac{\lambda_o}{2} \tag{18}$$

By combining equations (17) and (18) it results:

$$h \geq \frac{\lambda_o}{(n_e - n_o)\left(\sqrt{1-\frac{\sin^2 i_{min}}{n_o^2}} - \sqrt{1-\frac{\sin^2 i_{max}}{n_o^2}}\right)} \tag{19}$$

The technique proposed for the determination of the main refactive indices and the birefringence was also applied to characterize uniaxial crystals cut perpendicularly on the optical axis [14,15]. The information contained in [13] were published in a medical journal [16] due to their applicability in characterizing the anisotropy of the transparent biological tissues.

6. Conculsions

In this paper we have shown the possibility of using the equations (6)-(12) in order to determine the main refractive indices, the birefringence (including its sign) and the thickness of a uniaxial anisotropic layer of a nematic liquid crystal, having its director oriented parallel to the plane of the microscope stage (planar orientation), by processing the conoscopic interference images obtained with the polarizing microscope.

The proposed technique can be used for studying the optical anisotropic properties (main refractive indices and linear birefringence) and to determine the thickness values of the uniaxial anisotropic crystals or other anisotropic layers (such as stretched polymer foils).

References

[1] Ch.Y. Gao, H.R. Xia, J.Q. Xu, Sh.Ch. Si, H.J. Zhang, J.Y. Wang, H.L. Song, Cryst. Res. Technol., **42(11)**, 1126 (2007).
[2] Born, M. & Wolf, E. Principles of Optics. Cambridge University Press, England, 1999.
[3] R. E Wilcox, American Mineralogist **44**, 1272 (1959).
[4] F. D. Bloss, The spindle stage, Cambridge University Press, Great Bretagne,1981.
[5] L. A. Pajdzik, A. M. Glazer, J. Appl. Cryst., **39**, 326 (2006).
[6] M. A. Geday, W. Kaminsky, J. G. Lewis, A. M. Glazer, Journal of Microscopy **198**, 1 (2000).
[7] W. Kaminsky, K. Claborn, B. Kahr, Chemical Society Reviews, **33**, 514 (2004).
[8] D. O. Dorohoi, M. Postolache, M. Postolache, Journal of Macromol. Sci. – Physics. **B 40(2)**, 239 (2001).
[9] S. Picoş, G. Amarandei, I. Diaconu, D.O. Dorohoi, J. Optoelectron. Adv. Mater. **7**(2), 787 (2005).
[10] B. Kamb, American Mineralogist. **55**, 767 (1970).
[11] B. Kamb, American Mineralogist. **56**, 327 (1971).
[12] R.E. Stroiber, S.A. Morse, Crystal identification with the polarizing microscope. Chapman & Hall, USA,1994.
[13] G. Sharma, Digital color imaging handbook. CRC Press, 2003.
[14] L. Dumitrascu, I. Dumitrascu, O.D. Dorohoi, M. Toma, Optics Express, **16(25)**, 20884 (2008).
[15] L. Dumitrascu, I. Dumitrascu, O.D. Dorohoi, J. of Applied Crystallography, **421**, 878 (2009).
[16] L. Dumitrascu, I. Dumitrascu, D.O. Dorohoi, M. Toma, Virtual Journal for Biomedical Optics, Ed. W.F. Gregory, **4(2)**, 102 2009.